



1 **Discriminating fluvial fans and deltas: Channel
2 network morphometrics reflect distinct formative
3 processes**

4

5 Luke Gezovich^{1*}, Piret Plink-Björklund¹, Jack Henry^{1,2}

6 ¹ Colorado School of Mines, Geology & Geologic Engineering, 1500 Illinois Street, Golden, CO, 80401

7 ² Rice University, Earth, Environmental and Planetary Sciences, 6100 Main St., Houston, TX, 77005-
8 1827

9

10 *Correspondence to:* Luke Gezovich (lukegezovich@mines.edu)

11

12 **Abstract**

13 Recent recognition of a new type of fluvial system – fluvial fans – introduces a fan-shaped channel
14 network that appears similar to that of river-dominated deltas. Deltas form where rivers enter lakes and
15 oceans, while fluvial fans are terrestrial landforms. However, fluvial fans can reach the shorelines of
16 oceans or lakes, and in such cases the distinction between fluvial fan and river-dominated delta channel
17 networks become ambiguous. We currently lack fundamental understanding of these two landforms'
18 morphometric differences, despite their high socioeconomic significance, vulnerability to natural hazards,
19 and key differences in how these landforms respond to global climate change and urbanization. Here we
20 review the relevant conceptual differences in delta and fluvial fan network morphodynamics, propose a
21 set of quantitative morphometric criteria to distinguish fluvial fan and delta channel networks, and test
22 these criteria on 40 deltas and 40 fluvial fans from across the world. This initial attempt to distinguish
23 deltas and fluvial fans demonstrates that quantifying channel network angles, and trends in normalized
24 channel widths and lengths provides efficient criteria, but some ambiguities remain that need to be
25 resolved in future work. This research advances our mechanistic understanding of fluvial fan and delta
26 channel networks and the recognition of modern and ancient landforms on Earth and other planetary
27 bodies, such as Mars and Saturn's moon Titan.

28

29 **Plain Language Summary**

30 Fluvial fans are a newly recognized type of river system that look like river deltas, especially
31 when they reach lakes or oceans. This study explores how to tell them apart by measuring the size and
32 layout of channels in these fan-shaped landforms. Understanding these differences helps to predict how
33 these landforms respond to climate change and urbanization, and identify them on Mars and other
34 planetary bodies.

35

36



37 **1. Introduction**

38 River deltas are depositional landforms that form where rivers enter lakes or oceans. They are
39 home to over half a billion people, host abundant and biodiverse ecosystems, and function as both
40 economic and agricultural hubs (Saito et al., 2007; Tejedor et al., 2015). The form and function of deltas
41 is intimately linked to the evolving structure of their channel networks that determine how deltas
42 distribute sediment and nutrients (Passalacqua, 2017; Pearson et al., 2020; Tejedor et al., 2017). Delta
43 channel network morphology results from an intricate balance between sediment erosion and deposition
44 from river, tide, and wave energy fluxes. River fluxes create distributary channels and islands, tides
45 roughen the shoreline and widen the channels, and waves smooth the shoreline and decrease the number
46 of distributary channels (Broaddus et al., 2022; Galloway, 1975; Nienhuis et al., 2015, 2018; Paniagua-
47 Arroyave & Nienhuis, 2024; Vulis et al., 2023). Deltas dominated by river energy fluxes (river-dominated
48 deltas) (Galloway 1975; Nienhuis et al 2015; 2018; Broaddus et al 2022; Vulis et al 2023; Paniagua-
49 Arroyave and Nienhuis 2025) characteristically form fan-shaped landforms with complex distributary
50 channel networks (Fig. 1). In these deltas, channel network topology is defined by mouth bar deposition
51 and consequent distributary channel bifurcation (Bates, 1953; Edmonds & Slingerland, 2007; Wright,
52 1977).

53 Fluvial fans are another type of fan-shaped landform with channel networks that share
54 morphological similarities with the river-dominated delta channel networks (Fig. 2). Fluvial fans are a
55 relatively newly acknowledged type of fluvial landform (Weissman et al., 2010; Ventra & Clarke, 2018),
56 that forms via river avulsions or “channel jumps” across low-gradient floodplains (Chakraborty et al.,
57 2010; Martin & Edmonds, 2023; North & Warwick, 2007). Rivers have been traditionally regarded as
58 sediment transfer or bypass zones in source-to-sink systems (Allen, 2008; Fielding et al., 2012), whereas
59 fluvial fans are net depositional and build significant stratigraphic thicknesses (Chakraborty et al., 2010;
60 Moscariello, 2018; Weissmann et al., 2015). Fluvial fans are also called “wet” fluvial-dominated alluvial
61 fans (Schumm, 1977), megafans (Singh et al., 1993), or distributive fluvial systems (DFS) (Weissman et
62 al., 2010). Fluvial fans are distinct landforms from alluvial fans – which form by a combination of
63 gravitational and streamflow processes, feature steep gradients (typically 2–12°), and have a relatively
64 small radius typically less than 10 km (Blair & McPherson, 1994; Moscariello, 2018). Fluvial fans form
65 some of the largest terrestrial landforms on Earth (10^3 – 10^5 km 2 in surface area) (Horton & Decelles, 2001;
66 Leier et al., 2005) and have low gradients (typically 0.03–0.001°) (Brooke et al., 2022). Fluvial fans are
67 abundant across Earth, and they form in diverse climatic and tectonic settings (Hartley et al., 2010;
68 Weissman et al., 2010; Ventra & Clarke, 2018). Like deltas, fluvial fans are home to hundreds of millions
69 of people, and these highly dynamic landforms are critical for their livelihood – supporting agriculture,
70 fisheries, and freshwater access. For example, the Kosi fluvial fan experiences catastrophic river floods



71 that lead to large numbers of casualties and displaced populations (Sinha, 2009; Syvitski & Brakenridge,
72 2013), but also provides water and nutrients contributing to agricultural productivity and the overall
73 health of the ecosystem (Gupta et al., 2021).

74 While fluvial fans are terrestrial landforms, they can reach the shorelines of oceans (Fig. 2b) or lakes
75 (Figs. 2a, 2d and 2i). It is in such cases fluvial fan and river-dominated delta channel network distinction
76 becomes ambiguous, while wave-and tide-dominated deltas have distinctly recognizable morphologies
77 (Broaddus et al., 2022; Galloway, 1975; Nienhuis et al., 2015; 2018; Paniagua-Arroyave & Nienhuis,
78 2024; Vulis et al., 2023). We currently lack quantitative morphometric criteria for distinguishing river-
79 dominated delta and fluvial fan channel networks, despite their socioeconomic significance, key
80 differences in their natural hazard vulnerabilities, and in how they respond to global change. Deltas are
81 global change hotspots highly vulnerable to urbanization and climate change which can aggravate coastal
82 hazards and cause sea level rise (e.g., Syvitski et al., 2009; Giosan et al., 2014), and reduce sediment
83 supply due to river damming and artificial levees causing the drowning of deltas (e.g., Blum & Roberts,
84 2009; Syvitski et al., 2009; Giosan et al., 2014; Nienhuis et al., 2020; Paola et al., 2011).

85 Numerous fan-shaped landforms with channel networks have also been identified on other
86 planetary bodies such as Mars (Ori et al., 2000; Wood, 2006; Malin & Edgett, 2015) and Saturn's moon
87 Titan (Wall et al., 2010; Witek & Czechowski, 2015; Radebaugh et al., 2018). Deltas on planetary bodies
88 are important indicators of paleo-shorelines and have been utilized to reconstruct the shorelines and water
89 levels of ancient lakes and oceans on Mars (di Achille & Hynek, 2010). However, Martian paleo-ocean
90 shoreline reconstructions have so far yielded mixed results (De Toffoli et al., 2021). This discrepancy
91 could perhaps arise because shoreline-bound deltas have not been effectively distinguished from fluvial
92 fans on Mars, which may form thousands of kilometers inland from shorelines (Bramble et al., 2019;
93 Limaye et al., 2023; Tebolt & Goudge, 2022). Deltas also offer attractive targets for mission sites in
94 search of life due to their habitability and high biosignature preservation potential, as exemplified by the
95 selection of Jezero Crater for NASA's *Perseverance* rover, *Ingenuity* helicopter, and future Mars Sample
96 Return mission (Farley et al., 2020). Distinguishing deltaic and fluvial fan paleo-channel networks on
97 other planetary bodies is even more ambiguous, especially if the lakes and oceans are no longer present.

98 Over time, the accumulation of biogenic and sedimentary materials distributed via channel networks
99 contributes to the construction of stratigraphy. Fluvial fans and deltas are net depositional systems, as
100 both are characterized by spatially diminishing water surface slopes that reduce sediment transport
101 capacity, thereby producing spatiotemporal convergence and deposition of sediment (Ganti et al., 2014).
102 Consequently, in addition to their socioeconomic significance, both landforms significantly contribute to
103 the stratigraphic record, and their deposits can be used to decipher past environmental conditions. High
104 deposition rates in fluvial fans and deltas promote the preservation of environmental change signals in the



105 sedimentary record (Trampush & Hajek, 2017). Similar to modern river-dominated deltas and fluvial
106 fans, we lack morphometric criteria to distinguish these two fan-shaped channel networks in the
107 sedimentary record, such as in seismic datasets.

108 This study is motivated by developing quantitative morphometric distinction criteria for fluvial fan
109 and river-dominated delta channel networks. Prior work has established quantitative morphological
110 criteria for describing deltaic channel networks and linked these characteristics to theory (Chen et al.,
111 2021; Coffey & Shaw, 2017; Edmonds et al., 2011; Edmonds & Slingerland, 2007; Fagherazzi et al.,
112 2015; Ke et al., 2019; Passalacqua, 2017; Pearson et al., 2020; Tejedor et al., 2015, 2017). However, there
113 are no existing quantitative criteria to characterize fluvial fan channel networks or to differentiate the two
114 landforms. To develop such criteria, we review the relevant conceptual differences in delta and fluvial fan
115 network morphodynamics, propose quantitative morphometric criteria to distinguish fluvial fan and delta
116 channel networks, and test these criteria on 40 deltas and 40 fluvial fans (Supplementary Data) from
117 across the globe (Fig. 3). We test the robustness of the approach by analyzing differences in channel
118 network morphometrics concerning the size and gradient of the systems, hydroclimate conditions, lake
119 versus ocean terminations and tide- versus wave-influences in deltas, and channel morphology in fluvial
120 fans. We assess how effectively the proposed methods distinguish fluvial fans from river-dominated
121 deltas and examine why this distinction matters under global change. This work serves to improve our
122 mechanistic understanding of fluvial fan and delta evolution, and their accurate recognition on Earth,
123 other planetary bodies and in the sedimentary record.

124

125 **2. Delta and Fluvial Fan Channel Network Morphodynamics**

126 The nature of channel networks is dependent on distinct morphodynamic processes responsible for
127 their formation (Edmonds & Slingerland, 2007; Fagherazzi et al., 2015; Tejedor et al., 2015). Below we
128 analyze differences in delta and fluvial fan morphodynamics and review existing morphometric criteria
129 for quantifying deltaic distributary channel networks. Our review is not comprehensive; rather, it focuses
130 on the specific processes which govern the formation of the morphometric characteristics that we can then
131 use for distinction of these two landforms, namely channel network angles, and downstream changes in
132 channel widths and lengths. There are other important characteristics of deltaic channel networks, linked
133 to water and sediment discharge distribution, entropy, and connectivity (Chen et al., 2021; Ke et al., 2019;
134 Passalacqua, 2017; Pearson et al., 2020; Tejedor et al., 2015, 2017). These aspects are not considered in
135 this review, because they are outside the scope of this study that seeks to distinguish deltaic and fluvial
136 fan channel networks using easily applicable morphometric criteria that can be used to both deltaic and
137 fluvial fan networks.



138 We use the terms bifurcation and avulsion as *processes* rather than a geomorphological feature of
139 channel splitting. *Bifurcation* is the process of channel splitting driven by mouth bar formation (Edmonds
140 & Slingerland, 2007). *Avulsions* are channel “jumps”, where a channel changes its course due to channel
141 super-elevation or a more favorable (steeper) gradient at channel flanks (Gearon et al., 2024). Partial
142 avulsions split channels; however the process is distinct from *bifurcation* around a mouth bar.

143 **2.1 River Deltas**

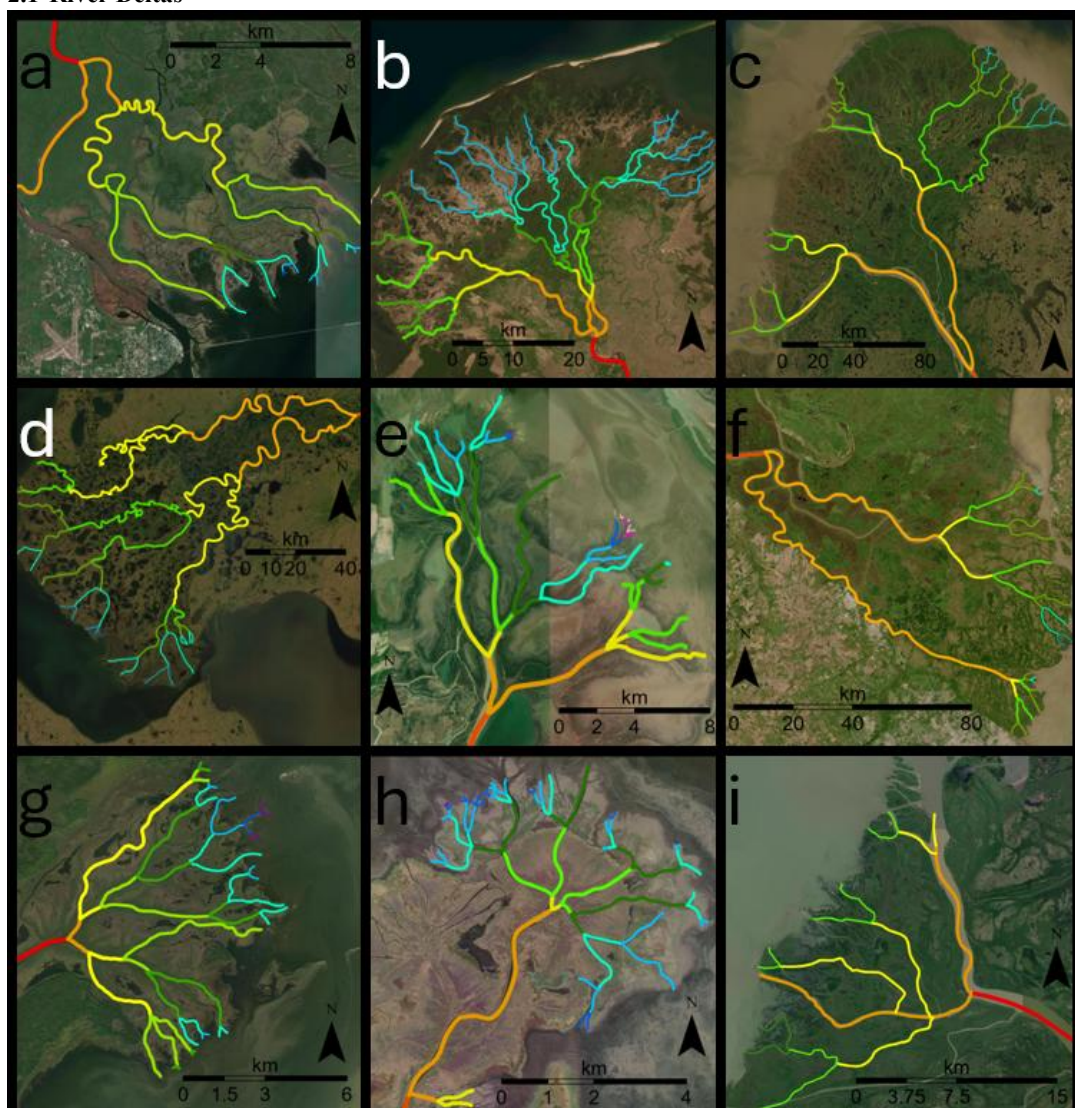


Figure 1: Examples of delta channel networks: (a) Apalachicola, (b) Selenga, (c) Yukon, (d) Kobuk, (e) Poyang Lake, (f) Parana (g) Saskatchewan, (h) Mamawi lake, (i) Slave deltas. The colors indicate channel hierarchy (see Methods). Base imagery from Esri's World Imagery basemap (© Esri, Maxar, Earthstar Geographics, and the GIS User Community).



144 Deltas (Fig. 1) always form where the mouth of a river enters a standing body of water. Here, the
145 transport capacity of the turbulent jet decreases, and the “parent” stream jet flow experiences both lateral
146 and bed friction, causing the flow to decelerate and rapidly expand laterally (Bates, 1953; Wright, 1977;
147 Edmonds & Slingerland, 2007; Jerolmack & Swenson, 2007). As a result, the transport capacity of the
148 turbulent jet decreases and sediment is deposited as a mouth bar basinward of the river mouth (Edmonds
149 & Slingerland, 2007). The process of mouth bar deposition and growth eventually leads to the bifurcation,
150 or downstream branching of a single (parent) channel into two daughter channels (Axelsson, 1967;
151 Coffey & Shaw, 2017; Edmonds & Slingerland, 2007) (Fig. 4a). These daughter channels are separated
152 by an island or shallow bay where sediment transport is significantly reduced or nonexistent, and flow is
153 unchannelized (Coffey & Shaw, 2017). Mouth bar deposition and resultant channel bifurcation repeat
154 multiple times leading to the seaward advancement of the shoreline and the construction of a delta
155 distributary channel network (Olariu & Bhattacharya, 2006; Edmonds & Slingerland, 2007) (Fig. 4a).

156 Deltas also experience channel avulsions at the lobe-level (Slingerland & Smith, 2004). These deltaic
157 avulsions occur within a region of high-water surface slope variability caused by backwater
158 hydrodynamics that are characterized by spatial flow deceleration and deposition during low flows, and
159 flow acceleration and bed scour with high flows (Lamb et al., 2012; Chatanantavet & Lamb, 2014). As
160 the backwater zone sets the location for avulsion in deltas (Chatanantavet et al., 2012), they are strongly
161 controlled by hydrodynamics in their receiving basin like bifurcations. As a result, the delta lobe size is
162 generally consistent and the lobe avulsion node migrates downstream commensurate with shoreline
163 progradation (Ganti et al., 2014). These avulsions episodically rearrange the depocenter at the delta lobe
164 scale, whereas the substantially more frequent bifurcations generate the topology of the delta distributary
165 channel networks (Edmonds & Slingerland, 2007; Bentley et al., 2016).

166 Resultant delta channel networks have a specific angle at which distributary channels bifurcate (Fig.
167 4a) (Coffey & Shaw, 2017), because a channel bifurcation will grow toward an equilibrium angle of 72°
168 to maximize flux at the two channel tips (Coffey & Shaw, 2017; Devauchelle et al., 2012; Ke et al., 2019;
169 Mahon et al., 2024). First described in tributary networks, this theoretical angle arises from diffusive
170 groundwater flow (Devauchelle et al., 2012). Testing of this concept reports bifurcation angles of $70.4^\circ \pm$
171 2.6° ($n = 9$) in natural deltas (Coffey & Shaw, 2017), and $68.3^\circ \pm 8.7^\circ$ ($n = 21$) (Coffey & Shaw, 2017)
172 and $74.1^\circ \pm 7.7^\circ$; ($n = 13$) (Federici & Paola, 2003) in experimental deltas.

173 The deltaic channel networks tend to consistently self-organize (Fagherazzi et al., 2008; Edmonds et
174 al., 2011) and exhibit a theoretical fractal pattern of decreasing channel widths and lengths associated
175 with increasing bifurcation order (Edmonds et al., 2011; Edmonds & Slingerland, 2007; Hariharan et al.,
176 2022; Seybold et al., 2017; Wolinsky et al., 2010) (Fig. 4a). The channel width trends align with
177 hydraulic geometric scaling: as the discharge of a parent channel divides into the discharge for two



178 resultant daughter channels, the daughter channel dimensions decrease as they scale with bankfull
179 discharge (Edmonds & Slingerland, 2007). Channel lengths decrease downstream with each successive
180 bifurcation because the jet momentum flux and consequent average grain transport distance decrease
181 downstream, causing new mouth bar deposition and accompanying bifurcations to occur closer to the
182 previous bifurcation node for a given channel (Edmonds & Slingerland, 2007) (Figs. 4a and 5a).

183 The nature of delta channel networks is further affected by waves and tides (Jerolmack & Swenson,
184 2007; Geleyne et al., 2011; Broaddus et al., 2022), where the relative strength of river, wave, and tide
185 processes determines whether deltas are river, wave, or tide dominated (Galloway, 1975; Nienhuis et al
186 2015, 2018; Nienhuis et al., 2020a; Vulis et al 2023; Paniagua-Arroyave and Nienhuis, 2025). Since wave
187 and tide-*dominated* deltas exhibit distinct morphologies from river-dominated delta and fluvial fan
188 channel networks, they are not considered in this study.

189 **2.2 Fluvial Fans**

190 In contrast to deltas where bifurcations and avulsions are strongly controlled by hydrodynamics
191 near a receiving basin of standing water (Chatanantavet et al., 2012; Ganti et al., 2014), fluvial fan river
192 avulsions are driven by a topographic slope break (Ganti et al., 2014; Martin and Edmonds, 2023).
193 Increased likelihood of avulsions at the fan apex is a consequence of the gradient reduction that triggers
194 in-channel sediment aggradation (Parker et al., 1998). These avulsions result from high channel bed
195 aggradation rates that are considerably higher than on the surrounding floodplains (Pizzuto, 1987). This
196 process causes river channel superelevation which ultimately triggers river avulsions near the fan apex
197 (Bryant et al., 1995; Mohrig et al., 2000; Gearon et al 2024). Since this slope break controls the location
198 of the fluvial fan's apex, the avulsion node is thus topographically pinned (Ganti et al., 2014). Partial or
199 full avulsions do occur further downfan, involving local gradient or discharge decreases, or crevassing
200 processes (Assine, 2005; Chakraborty et al., 2010; Donselaar et al., 2013; Gearon et al 2024) (Fig. 2).
201 Fluvial fan channel networks result from repeated avulsions that superimpose new channel positions on
202 paleo-channel locations and split channels by partial avulsions and crevasses. This generates apparent
203 channel “bifurcations” (North & Warwick, 2007) (Fig. 4b). However, as a process these are not
204 bifurcations related to mouth bar deposition but rather generated by avulsions. Fluvial fan channel
205 networks are predominantly paleochannel networks rather than active channel networks like in deltas
206 (North & Warwick, 2007; Chakraborty et al., 2010). Multiple channels can actively transmit discharge at
207 partial avulsions, such as during major river floods.

208

209

210

211

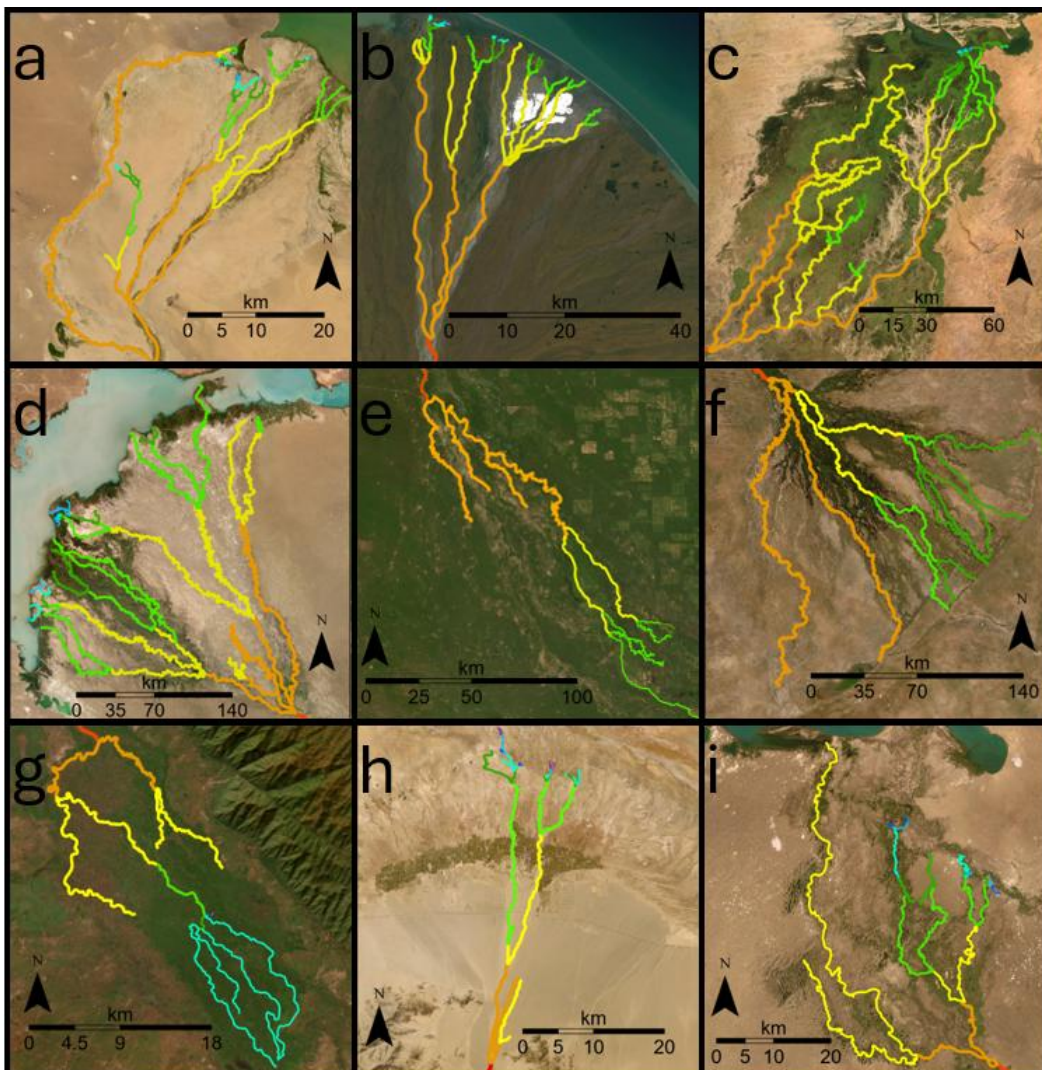


Figure 2: Examples of fluvial fan channel networks: (a) Dzavhan Gol, (b) Kongakut, (c) Niger, (d) Ili, (e) Pilcomayo, (f) Okavango, (g) Shire, (h) Nomon He, and (i) Aksu fans. The colors indicate channel hierarchy (see Methods). Base imagery from Esri's World Imagery basemap (© Esri, Maxar, Earthstar Geographics, and the GIS User Community).

212 Downstream decrease in channel width has been documented in modern and ancient fluvial fans
213 (Nichols, 1987; Kelly & Olsen, 1993; Nichols & Fisher, 2007; Weissman et al., 2010; Davidson et al.,
214 2013; Owen et al., 2015; Wang & Plink-Björklund, 2019), linked to discharge losses to floodplain
215 processes, infiltration into the loose sediments of the fan, and evapotranspiration (Horton & Decelles,
216 2001; Hartley et al., 2010; Weissman et al., 2010; Davidson et al., 2013). However, some fluvial fan



217 channels have also been shown to widen downstream, possibly due to changes in channel planform or
218 aspect ratio, discharge contribution from groundwater, or discharge capture from adjacent rivers
219 (Chakraborty et al., 2010; Davidson et al., 2013). Fluvial fan channel networks have been studied for
220 qualitative descriptions of channel planform morphology (Davidson et al., 2013; Hartley et al., 2010;
221 Weissman et al., 2010), and scaling relationships (Davidson et al., 2013; Davidson & Hartley, 2014).
222 Modeling establishes a relationship between the fluvial fan shape and avulsion dynamics, such as
223 avulsion trigger period and abandoned channel dynamics (Edmonds et al., 2022; Martin & Edmonds,
224 2023).

225 Fluvial fans are distinct landforms from alluvial fans that feature steep gradients (typically 2–
226 12°), have a relatively small radial distance typically less than 10 kilometers, and lack channel networks
227 (Blair & McPherson, 1994; Moscariello, 2018). Although surface channels may occur on alluvial fans,
228 these are transient features formed by surface erosion, and do not construct alluvial fans which form by a
229 combination of gravitational and sheet flood processes (Blair & McPherson, 1994; Moscariello, 2018).
230 Thus, alluvial fans are not considered here as they are distinct from fluvial fan channel networks that form
231 by river avulsions.

232 **2.3 Morphometric Criteria for Recognition of Delta and Fluvial Fan Channel Networks**

233 Based on the above differences in delta and fluvial fan morphodynamics, we hypothesize that the
234 morphometric differences in their channel networks can be quantified. Based on prior work, we expect
235 river-dominated delta channel networks to display downstream decreasing channel widths and lengths
236 with increasing bifurcation order (Edmonds & Slingerland, 2007; Seybold et al., 2007; Wolinsky et al.,
237 2010), and have an average channel network angle of approximately 72° (Coffey & Shaw, 2017). These
238 metrics should differ in fluvial fans, because the channel networks are built by avulsions rather than
239 bifurcations. However, also delta networks experience avulsions and we expect some overlap in the
240 network angles. Below, we test these morphometric criteria on 40 river-dominated delta and 40 fluvial fan
241 channel networks (Fig. 3).

242

243 **3. Dataset and Methods**

244 Although automated channel mapping tools like ChannelExtractor in TopoToolbox (Schwanghart
245 & Kuhn, 2010) and Rivamap (Isikdogan et al., 2017) exist, these existing methods rely on either terrain-
246 based flow routing or the detection of active surface water – typically based on spectral characteristics –
247 to delineate river channels. However, fluvial fan channel networks are predominantly composed of
248 paleochannels that lack both clear topographic expression and surface water signatures. Both delta and
249 fluvial fan channels can also be only a few meters wide, often falling below the spatial resolution of
250 commonly available DEMs and remote sensing imagery. In such settings, the coarse resolution and



251 smoothing of subtle terrain in DEMs, especially in low-relief environments, further limit the effectiveness
252 of automated extraction. As a result, we are constrained to manual digitization, as described below.

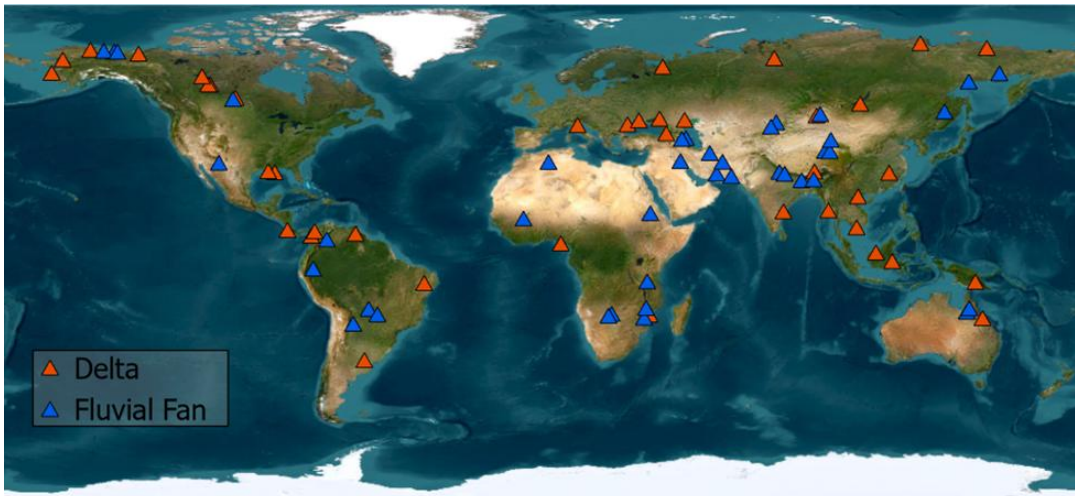


Figure 3: Map of deltas and fluvial fans in this study. Base imagery from Esri's World Imagery basemap (© Esri, Maxar, Earthstar Geographics, and the GIS User Community).

253 **3.1 Channel Order**

254 To establish channel order in networks, we follow Dong et al. (2016). Their method follows a
255 simple rule: bifurcations produce downstream increasing channel order through channels that branch. To
256 be considered a channel of a higher order, the resultant channels must not merge downstream. When a
257 first-order channel bifurcates, two second-order channels develop downstream of this bifurcation. When
258 these two channels subsequently bifurcate, two new pairs of third-order channels form, and so on (Figs.
259 4a and 4b). Identification of bifurcation nodes follows Edmonds et al. (2011), such that the first-order
260 bifurcation for a river channel is the first bifurcation that the channel undergoes (Fig. 4a). Although these
261 methods were developed for deltaic channel networks, here we adapt them for fluvial fan networks also
262 (Figs. 4c and 4d). We do not consider channels that loop or rejoin downstream, or channels of non-fluvial
263 origin, such as tidal channels or inlets (e.g., Smart, 1971; Tejedor et al., 2015) that are not connected to
264 the fluvial distributary channels.

265 **3.2 Channel Length and Width Measurements**

266 Channel length and width measurements follow Edmonds and Slingerland (2007), where channel
267 length is measured as the distance between two bifurcation nodes in deltas (Fig. 4a). We adopt this
268 methodology also to fluvial fans to measure channel lengths between avulsion nodes (Fig. 4c). The
269 average width of a channel segment is recorded from three separate width measurements: one
270 immediately after a node (w_i), one immediately before the next node (w_f), and one halfway between these
271 two points at the midpoint of the channel segment (w_h) (Figs. 4a and 4c). Channel width measurements



272 were not performed in locations where a channel has locally split into multiple branches that join
273 downstream. In deltas, channel width measurements were recorded based on the width of water present in
274 the channel, as observed in the satellite imagery. For fluvial fans, paleo-channel width measurements
275 were based on the bankfull width, defined by clearly visible channel banks or vegetation boundaries. All
276 channel length and width measurements were normalized using the initial first-order channel width,

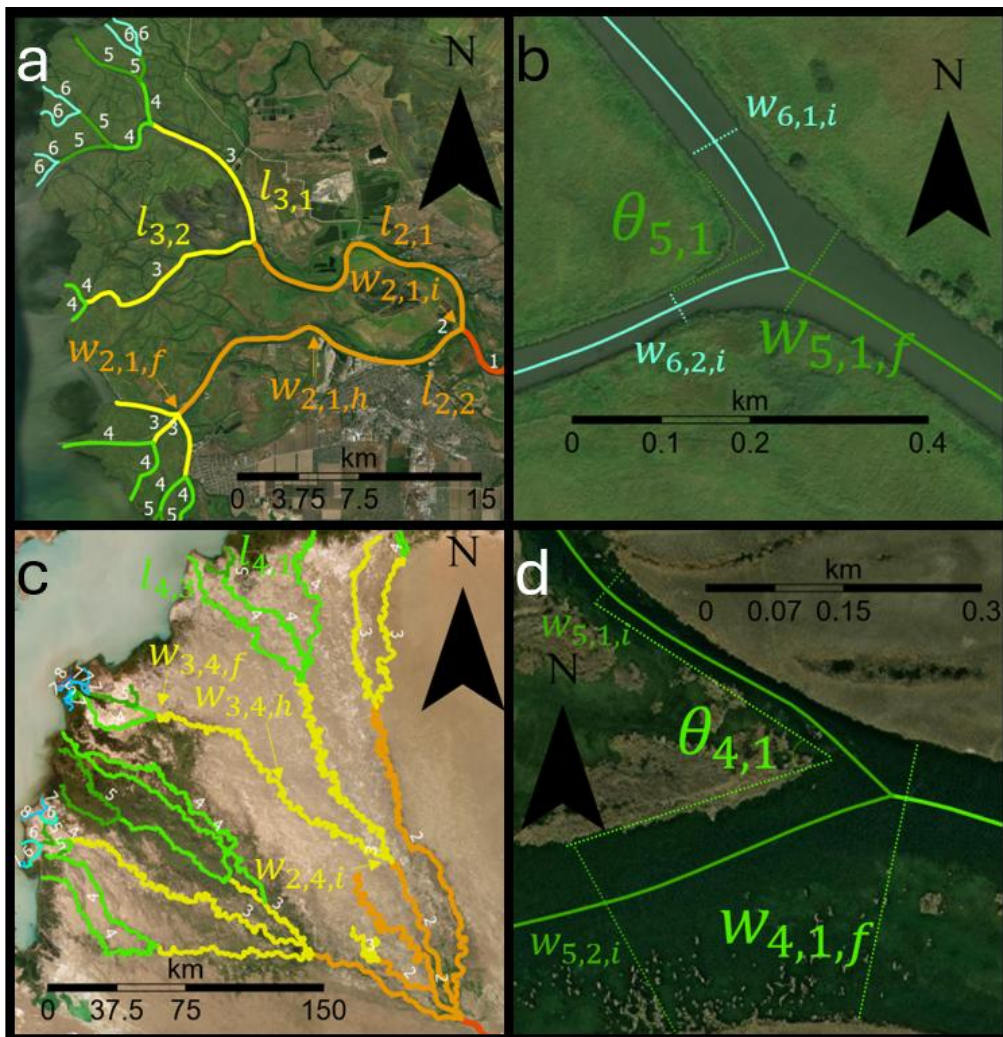


Figure 4: Illustration of (a) channel order, length, and width and (b) bifurcation angle measurements in deltas (Don delta). Illustration of (c) channel order, length, and width and (d) divergence/crossover angle measurement (Ili fan). Arrows point to locations of w_i = initial channel width, w_h = midpoint channel width, w_f = final width measurements. The w_f is set as the length of two limbs that track along the edges of the mouth bar. θ_n corresponds to the bifurcation or divergence/crossover order. Base imagery from Esri's World Imagery basemap (© Esri, Maxar, Earthstar Geographics, and the GIS User Community).



277 following the methodology of Edmonds & Slingerland (2007). Consequently, the normalized channel
278 width value for first-order channels is always equal to one. First-order channel lengths were measured
279 between the last occurrence of tributary channels and the first channel splitting node and contain no
280 significant value for our study.

281 **3.3 Network Angle Measurements**

282 To quantify network angles, we adopt the methodology of (Coffey & Shaw, 2017) developed for
283 measuring channel bifurcation angles, which determines the angles of mouth bars formed at the end of an
284 upstream channel. In this methodology, the final channel width directly upstream of a bifurcation (w_f) is
285 set as the length for two limbs of an angle that follows the mouth bar-water contact to measure a
286 bifurcation angle (θ_n) (Coffey & Shaw, 2017) (Fig. 4b). The same methodology is adapted here for fluvial
287 fans (Fig. 4d). In some river deltas, tidal processes cause bifurcation of a channel into three channels
288 instead of two; these are referred to as trifurcations (Leonardi et al., 2013), and a few such measurements
289 are included in the dataset in the very distal portions of deltas where tidal influence is significant. We do
290 not measure angles where channels loop or rejoin downstream of avulsions or bifurcations. In essence, we
291 focus on the morphology of branching channel networks and measure the visible angles between channels
292 or paleo-channels independent of their origin (Fig. 4b and 4d).

293 **3.4 Global Delta and Fluvial Fan Channel Network Database**

294 To test the applicability of the proposed criteria, we selected 40 river-dominated deltas and 40
295 fluvial fans (Fig. 3 and Supplementary Data). These landforms were selected from a diverse range of
296 hydroclimatic, topographic, and basinal conditions from across the world (Fig. 3). All deltas have been
297 identified as such by prior work (Broaddus et al., 2022; Galloway, 1975; Hartley et al., 2010; Leier et al.,
298 2005; Nienhuis et al., 2015, 2018; Vulis et al., 2023). The river dominance of deltas and the presence of
299 tide- or wave-influence was determined using the established principles of process-based delta
300 classification (Broaddus et al., 2022; Galloway, 1975; Nienhuis et al., 2015, 2018; Paniagua-Arroyave
301 and Nienhuis 2025; Vulis et al., 2023). All included deltas display active discharge based on satellite
302 imagery. Only river-dominated deltas are included in the dataset, because wave-and tide-dominated delta
303 morphology is distinct from that of fluvial fans. Many natural river-dominated deltas are, however, tide-
304 or wave-influenced to varying extents. We test the effects of tide- and wave-influence on the
305 morphometric criteria by comparative analyses. Fluvial fans were located using their apex coordinates
306 from the global fluvial fan database of Hartley et al. (2010). This database also includes data on fluvial
307 fan length, gradient, termination style, such as axial, contributory, lacustrine, marine, playa, desert/dune,
308 and wetland styles. Contributory termination refers to that a distributive paleo-channel pattern becomes
309 contributory at the fan toe, and axial to fans where the active channels form a confluence with another
310 river (Hartley et al., 2010). We also subdivided delta termination styles in lakes and oceans. To test the



311 robustness of our methodology, we analyze whether the landform size, gradient, termination style, or
312 wave- and tide-influence in deltas affect the results.

313 **3.5 Mapping with ArcGIS Pro**

314 Delta and fluvial fan channel networks were mapped using ArcGIS Pro software (Version 3.2.1)
315 (Fig. 1, 2, and 4). Two feature classes were created: one for deltas and one for fluvial fans. Each delta or
316 fluvial fan landform was then individually mapped as a shapefile layer under the corresponding feature
317 class. The shapefiles for channel networks were created as polyline features, which allow a user to
318 manually trace individual river channel segments while automatically recording line lengths. Channels
319 widths and angles were measured using the line and angle measurement tools in ArcGIS Pro. All data was
320 recorded in the attribute table for each landform. This data was then exported and organized into Excel
321 documents and subsequently converted to a python and pandas readable CSV files (Supplementary Data).

322 A limitation of our methodology is the uncertainty regarding how soon satellite images were
323 captured after a precipitation event for a given landform, which can significantly influence channel
324 discharge and affect measured channel widths, especially in arid fluvial fans. Such events can also
325 reactivate partial avulsions and crevasse, potentially increasing the apparent number of channels.
326 However, none of the selected systems exhibited observable seasonal or significant discharge changes
327 across their channel networks. Additionally, because this study relies on values normalized to the initial
328 channel width, the effects of seasonal variability on channel width measurements are minimized.

329 **3.6 Code and Statistics**

330 Kolmogorov-Smirnov and Shapiro-Wilk tests were first applied to determine whether the data is
331 normally distributed. Levene's test was used to test for differences in variances in populations which do
332 not exhibit a normal distribution (Trauth, 2006). Independent samples or Welch's T-test were then applied
333 to test for a difference in means for populations with similar and dissimilar variances, respectively, while
334 one-sample T-tests were used to test comparisons of a subgroup against the overall population mean
335 (Trauth, 2006). For this study, a p-value less than 0.05 (5% significance level) suggests that the two
336 population distributions, variances, or means are not similar. Data analyses confidence intervals were
337 calculated according to Mendenhall et al., (2012). Data analysis and visualization were performed using
338 Python. Open-source data visualization libraries Matplotlib (Hunter, 2007), NumPy (Harris et al., 2020),
339 SciPy (Virtanen et al., 2020) and Seaborn (Waskom, 2021) were utilized.

340

341 **4. Results**

342 **4.1 Delta and Fluvial Fan Channel Network Angles**

343 The average channel network angle (θ_d) in deltas is 73.8° with a 95th percentile confidence interval of
344 $\pm 1.9^\circ$ ($n = 528$) (Fig. 5a). The average channel network angle (θ_f) in fluvial fans is $55.0^\circ \pm 2.0^\circ$ ($n = 520$)



345 (Fig. 5b). The delta and fluvial fan network angle populations are not normally distributed according to
346 both Kolmogorov-Smirnov (KS) and Shapiro-Wilk (SW) tests, with p-values less than 0.05. Levene's test
347 for statistical difference in variances also results in a p-value less than 0.05, suggesting population
348 variances are statistically different. A subsequent independent samples T-test suggests the means of delta



349 and fluvial fan angle populations are statistically different, with a p-value less than 0.05. All statistical

350 results are recorded in Supplementary Table 1 in the Supplementary Information.

351

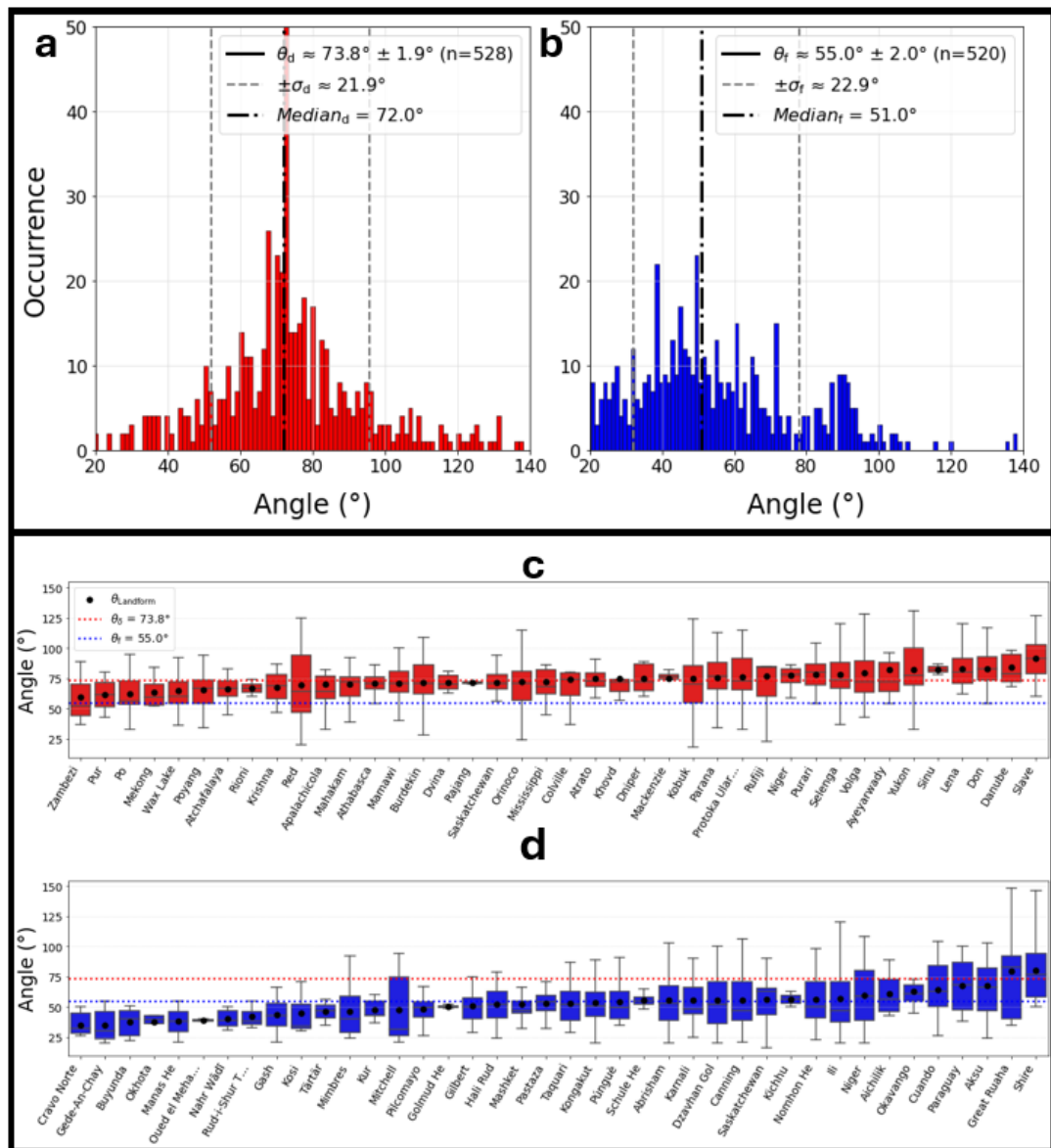


Figure 5: Histograms depicting distributions of (a) delta angles with average delta angle (θ_d), its standard deviation (σ_d) and median and (b) fluvial fan angles with average fan angle (θ_f), its standard deviation (σ_f), and median displayed. Box-and-whisker plot displaying the average angle for each delta (c) and fluvial fan (d) landform ($\theta_{Landform}$).



352 We also reviewed the average network angle of each individual delta and fluvial fan (θ_{landform}) (Figs.
 353 5c and 5d), and these analyses reveal some overlap. All fluvial fans have average angle values less than
 354 60°, except for six landforms, or 15% of fluvial fans in this study. Four of these landforms have average
 355 angles larger than 60° (60.8°, 63.2°, 67.7°, 67.9°), and two larger than the delta average of 73.7° (79.6°,
 356 80.1°). All individual deltas have average network angles larger than 60°, except for one delta (59.3°).
 357 There are also three deltas with average angles around 60° (61.5°, 62.4°, 63.3°).

358 The distribution of delta angles grouped by order (Fig. 6a) yields no strong trends for mean angle in
 359 deltas. Seventh and tenth order channels have slightly lower average angle values at 65° and 67°, but
 360 these higher-order groups have low sample sizes ($n = 3$; $n = 8$) (Fig. 6a). The distribution of fluvial fan
 361 angles grouped by order does yield a trend: the average angle for first through third orders (θ_1 , θ_2 , and θ_3
 362 in Fig. 6b) is between 47 – 50°, and increases to 61 – 63° for fourth through eight order channels, and to
 363 66° for ninth order angles ($n = 6$) (θ_4 – θ_9 , in Fig. 6b). In contrast to the unimodal distribution of delta
 364 angles, the distribution of higher-order fluvial fan angles is bimodal, with a dominant peak near 50° and a
 365 secondary peak around 80 – 100° (Fig. 6b).

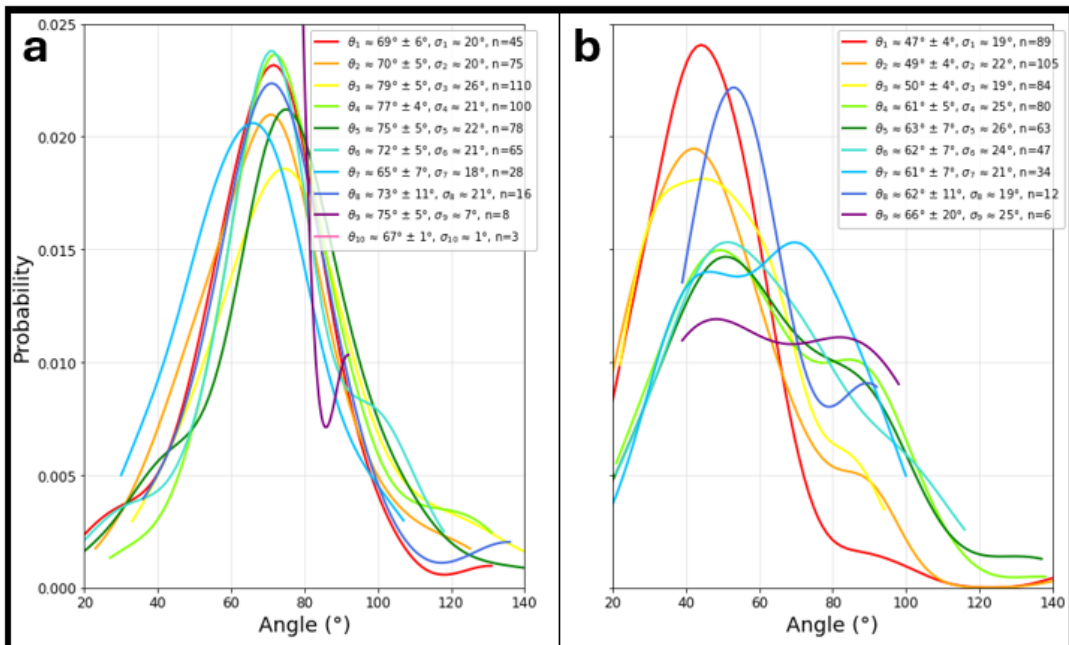


Figure 6: Distribution of (a) delta bifurcation angles, and (b) fluvial fan divergence/crossover angles grouped by order (θ_n) with the 95th percent confidence interval. (σ_n) = denotes standard deviation. n denotes sample size.

366 All deltas in this analysis are river-dominated deltas, however some are tide- or wave-influenced.

367 Grouping deltas by process regime shows that the average bifurcation angle for the 19 river-dominated



368 deltas (θ_R) is $73.4^\circ \pm 2.2$ (n = 375), for the 16 tide-influenced deltas (θ_t) $75.6^\circ \pm 3.9$ (n = 139) and for the
 369 5 wave-influenced deltas (θ_w) $67.1^\circ \pm 10.1$ (n = 14) (Fig. 7a). The river-dominated and tide-influenced
 370 delta angle means are not statistically different from the mean angle for the whole delta population
 371 (Supplementary Table 1). The wave-influenced delta angles were omitted from this statistical analysis due
 372 to a small sample size (n = 14 < 30).

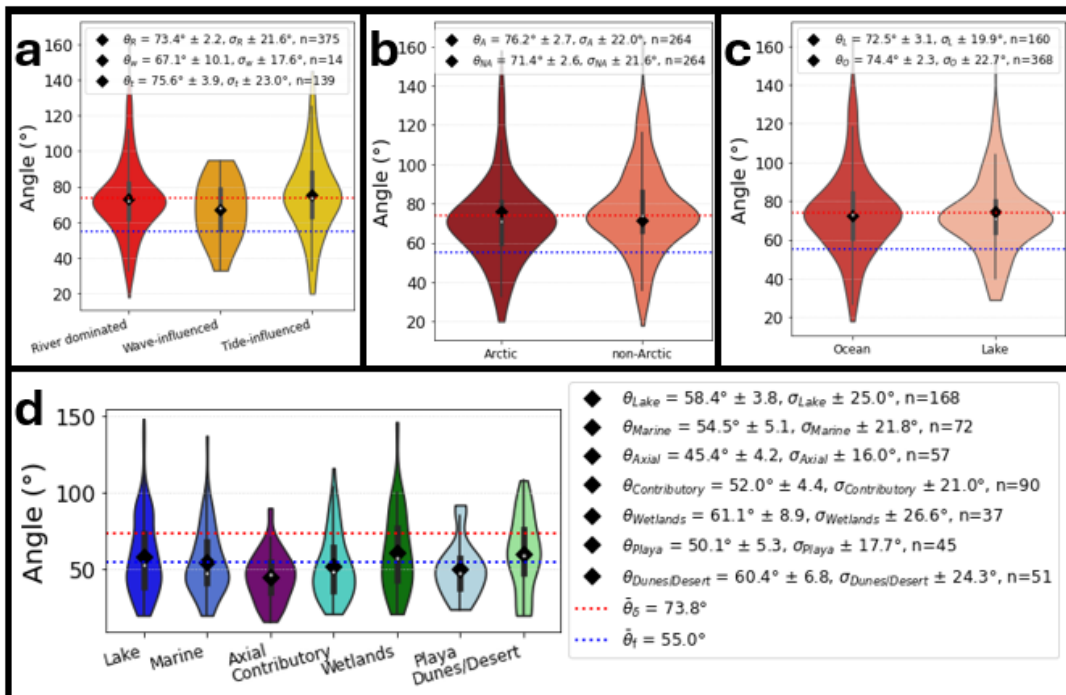


Figure 7: Violin plots depicting angle distributions for (a) delta process regime: river dominated (θ_R), wave-influenced (θ_w), and tide-influenced (θ_t), (b) deltas in non-Arctic (θ_{NA}) and Arctic (θ_A) climates, (c) ocean terminated deltas (θ_O) and lake terminating deltas (θ_L), and (d) fluvial fan termination styles. All average angle values have a corresponding 95th percent confidence intervals, standard deviation (σ), and sample count (n).

373 Many delta angle measurements in this dataset come from arctic deltas. The comparison between
 374 Arctic and non-Arctic deltas shows that Arctic deltas have a larger mean angle ($\theta_A = 76.2^\circ \pm 2.7$, n =
 375 264), than non-arctic deltas ($\theta_{NA} = 71.4 \pm 2.6$, n = 264) (Fig. 7b). There is a statistically significant
 376 difference in means between Arctic and non-Arctic deltas (Supplementary Table 1). Grouping deltas by
 377 termination style (Fig. 7c) shows that deltas which terminate in lakes have slightly smaller mean angles
 378 than those that terminate in oceans ($\theta_L = 72.5^\circ \pm 2.7$, n = 160 versus $\theta_O = 74.4^\circ \pm 2.6$, n = 160), but these
 379 differences are not statistically significant compared to the whole delta population (Supplementary Table
 380 1).

381 Grouping fluvial fans by their termination style shows some differences (Fig. 7d), where the mean



382 angles vary from a low of $\theta_{\text{Axial}} = 45.4^\circ \pm 4.2$ ($n = 57$) for axial-terminating fluvial fans to $\theta_{\text{wetlands}} = 61.1^\circ \pm 8.9$ ($n = 37$) for wetland terminating fans (Fig. 7d). All fluvial fan termination types, except for axial-terminating fans, exhibit population means that are statistically similar to the overall fluvial fan population (Supplementary Table 1). However, each termination style is represented by only 4 to 6 landforms, limiting the statistical power of comparisons and generalizations, despite the relatively robust measurement numbers in wetland ($n = 37$), playa ($n = 45$), dunes/desert ($n = 51$), and axial-terminating fans ($n = 57$). There also appears to be some discrepancies in Hartley et al. (2010) assignment of termination types. We also tested whether landform size (Supplementary Fig. 1) and gradient (Supplementary Fig. 2) affect the channel network angles, and these analyses yield no trends, supporting the robustness of our methodology.

392 **4.2 Channel Lengths and Widths**

393 Normalized channel length and width measurements reveal morphological differences between
394 fluvial fan and delta channels. Both landform types show non-linear decreases in these values with
395 increasing channel order (Fig. 8). Statistical analyses confirm that the overall means for normalized
396 channel length and width differ significantly between fluvial fans and deltas (Supplementary Table 1).
397 Fluvial fan channels are generally an order of magnitude longer than delta channels, with mean
398 normalized length of 147.09, compared to 17.18 in deltas (Figs. 8a and 8c). In contrast, delta channels
399 tend to be slightly wider, with normalized mean width of 0.40 compared to 0.26 in fluvial fans (Figs. 8b
400 and 8d).

401 Comparing the normalized dimensions by channel order (Fig. 9) shows further trends. The lower
402 order normalized channel widths (orders 1–5) in fluvial fans are significantly longer, and the channel
403 shortening rate is higher compared to deltas (Fig. 9a). The normalized lengths become very similar in
404 orders 7–8, and then diverge again for the higher orders where the fluvial fan channel lengths are
405 somewhat longer, but the channel shortening rates are higher in deltas. Normalized channel widths show
406 significant differences for orders 2–8, but not for 9–11. Only a few landforms have channels with orders
407 exceeding 9. Fluvial fan narrowing rates are very high from order 1 and 2, and very low in orders 7–10
408 (Fig. 9b). The narrowing rates are more uniform in deltas.

409 When comparing individual deltas by process regime, tide- and wave-influenced deltas have a
410 significantly higher mean normalized channel widths relative to the whole delta population
411 (Supplementary Fig. 3 and Supplementary Table 1).

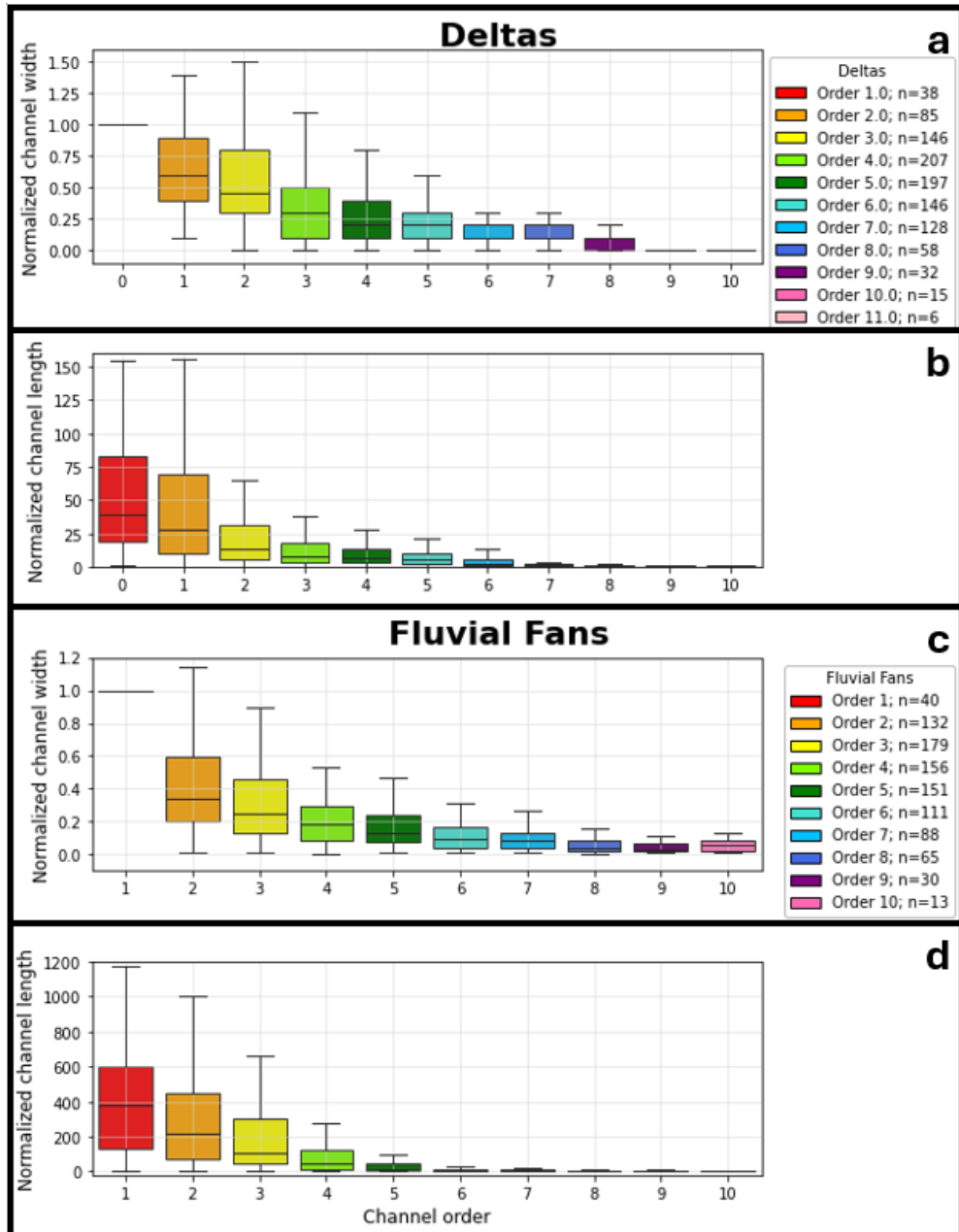


Figure 8: Box and whisker plots illustrating normalized delta channel widths (a) and lengths (b) and normalized fluvial fan channel widths (c) and length (d), plotted by channel order.

412

413

414

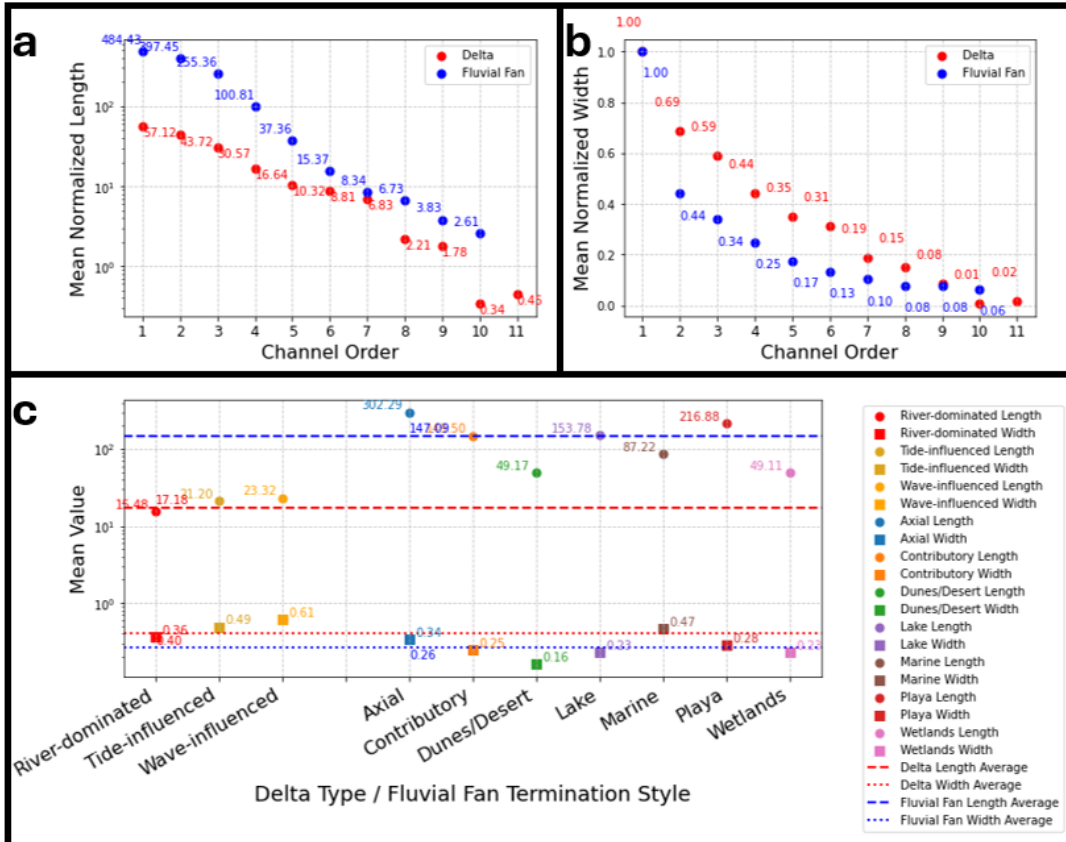


Figure 9: Mean normalized delta and fluvial fan channel (a) lengths by order and (b) width values by order. (c) Mean channel length and width values for different types of deltas and fluvial fan termination styles.

415 Comparison by fluvial fan termination styles, shows that axial and playa-terminating fans exhibit
416 longer mean normalized channel lengths compared to the whole fluvial fan population, whereas
417 dunes/desert, marine, and wetland-terminating fans have shorter mean lengths (Supplementary Fig. 3 and
418 Supplementary Table 1). Contributory and lake-terminating fans do not differ significantly from the
419 overall mean. Regarding normalized channel widths, axial and marine fans have wider channels, while
420 dunes/desert fans are narrower. Normalized width values for contributory, lake, playa, and wetland fan
421 channels show no difference from the whole population mean (Supplementary Fig. 3 and Supplementary
422 Table 1). Statistical analyses of channel length and width were not conducted for different fluvial fan
423 termination styles due to insufficient sample sizes ($n < 30$) in most categories.

424

425 5. Discussion



426 **5.1 Effectiveness of Morphometric Criteria in Distinguishing Deltas and Fluvial Fans**

427 The average channel network angles are distinctly different in deltas and fluvial fans by 20° , and
428 this statistically significant difference is a useful criterion in distinguishing these two landform types.
429 While some overlaps exist at the landform level, these cases are relatively limited, where 15% of fluvial
430 fans in this dataset have an average angle larger than 60° (Fig. 5d) and 10% of deltas have an average
431 angle less than 64° (Fig. 5c). These findings support the utility of average branching angle as a
432 distinguishing metric between deltas and fluvial fans, though some uncertainty remains, and additional
433 criteria are necessary for more robust distinction.

434 An additional criterion is the distribution of average angles by channel order, where fluvial fans
435 have increasing angles and a bimodal distribution in orders 4–8 (Fig. 6). Other supportive criteria may be
436 the differences in values and distributions of the normalized channel lengths and widths (Figs. 8 and 9),
437 but the low sample numbers do not allow us to test these criteria by individual landforms. A useful
438 criterion would be to link channel narrowing with the bifurcation and avulsion nodes. In deltas, the
439 downstream channel narrowing occurs in stepwise manner at the bifurcation nodes, whereas in fluvial
440 fans this decrease should be gradual and not linked to the node positions where full avulsions occur. Our
441 data was collected in a manner that does not allow us to do these analyses.

442 A potential source of overlap in the delta and fluvial fan channel network average angles is that
443 not all measured angles in deltas are bifurcation angles, as deltas also experience avulsions (e.g., Fig. 1e).
444 A closer inspection of the four deltas with low average network angles reveals that each contains very few
445 measurements ($n = 3$, $n = 4$, $n = 6$, $n = 7$). In these cases, the limited sample size allows the rarer avulsion
446 angles to affect the mean values more strongly.

447 Examining fluvial fans with high average angles shows that these are low-gradient wetland fans,
448 where the avulsion angles tend to be wider as a function of avulsion mechanisms (see Discussion below).
449 However, they may also suggest a methodological limitation. While the local avulsion angles in low-
450 gradient wetland fans are wide (measured the final channel width directly upstream of a bifurcation (w_f)
451 as the length for two limbs of an angle), angles between the longer channel reaches are considerably
452 narrower (Supplementary Fig. 4). We plan to further develop angle measurement methods to capture
453 both the local and the reach-scale angles in future work.

454 In summary, this initial attempt to distinguish deltas and fluvial fans demonstrates that
455 quantifying channel network angles, and trends in normalized channel widths and lengths provides
456 efficient criteria. However, we also show that sample sizes are important for accurate recognition of
457 landforms.

458 **5.2 Processes that determine delta and fluvial fan channel network angles**



459 While the 72° average bifurcation angle has a theoretical explanation in diffusion in non-channelized
460 flow (Coffey & Shaw, 2017), there is currently no established explanation for the approximately 55°
461 average network angle in fluvial fans. In deltas, bifurcation as a process is the product of sedimentation
462 from turbulent jets that form at the mouths of rivers entering basins (Bates, 1953; Coffey & Shaw, 2017;
463 Edmonds & Slingerland, 2007; Fagherazzi et al., 2015; Jerolmack & Swenson, 2007; Wright, 1977).
464 Once a mouth bar is formed, the flow through the distributary channel bifurcations can be modeled as
465 diffusive flow (Coffey & Shaw, 2017), and the resulting critical angle of 72° represents a stable
466 morphology for the bifurcation as it grows in a diffusive groundwater field (Devauchelle et al., 2012; Ke
467 et al., 2019). The slightly larger network angles in Arctic deltas may reflect environmental influences
468 such as ice cover, permafrost, or limitations on overbank flow (Lauzon et al., 2019; Piliouras et al., 2021;
469 Walker, 1998).

470 River avulsions are set up by channel superelevation (Mohrig et al., 2000), or when the slope down the
471 flanks of the channel provides a steeper descent than the existing river channel (Slingerland & Smith,
472 1998; Törnqvist & Bridge, 2002). Avulsions result from channel bed aggradation that reduces the channel
473 capacity (Bryant et al., 1995). Once an avulsion is triggered, and full or partial river flow exits the
474 channel, a new channel is generated by surface runoff erosion. Thus, the prevailing topographic gradient
475 would tend to keep the nearby flows more focused in a slope-parallel direction, compared to bifurcations,
476 resulting in narrower network angles compared to bifurcations (Fig. 5b).

477 The contrast between diffusion-dominated and surface runoff erosion-dominated processes in shaping
478 delta versus fluvial fan channel network topology is further supported by tributary channel network
479 analyses that originally defined the critical angle of 72° (Devauchelle et al., 2012). Tributary channel
480 network analyses show that the average tributary angle of 72° only occurs in humid catchments with high
481 groundwater recharge, where tributary networks are shaped by groundwater diffusion (Seybold et al.,
482 2017). In contrast, tributary network angles average at 45° in arid landscapes where surface runoff
483 dominates (Seybold et al., 2017), or are even lower in the driest catchments (Seybold et al., 2018).

484 Fluvial fan gradient decreases progressively downstream (e.g. Chakraborty et al., 2010), such that
485 higher gradients near the fan apex likely generate more acute angles, whereas the very low gradients near
486 the toe of the fan would allow for wider angles. This trend likely explains the downstream increase in
487 fluvial fan network angles and the emergence of the second, wider peak in higher order channels (Fig.
488 6b). Furthermore, avulsion mechanisms have been shown to change from channel superelevation in
489 upstream river reaches, where river gradients are steeper, to gradient advantage in downstream low-
490 gradient reaches (Gearon et al., 2024). In these low-gradient zones, crevassing processes can produce
491 high-angle deviations with the angle values around 90° (Rahman et al., 2022). Avulsion angles above
492 100° have been measured in meandering rivers on low-gradient floodplains with vegetation (see Rahman



493 et al., 2022). These effects may be important controls in the fluvial fan channel networks in low-gradient
494 vegetated wetlands. Reitz & Jerolmack, (2012) show that abandoned paleochannel reoccupation may
495 control new avulsion positions, and paleochannel density is highest in the narrower fan apex. Avulsion
496 angles may also change over time due to evolving channel width ratios (Morais & Montanher, 2022), or
497 may be affected by a critical angle or bend curvature (Yang, 2020).

498 We thus conclude that the distinction between deltaic and fluvial fan channel network angles arises
499 from the dominant formative processes: diffusive flow in deltas versus surface runoff erosion in fluvial
500 fans. Furthermore, in fluvial fans, network angles appear to be negatively correlated with surface
501 gradients, with lower gradients allowing for wider avulsion angles.

502 **5.3 Ancient deltas and fluvial fans**

503 Our proposed methodology could also be used to distinguish ancient fluvial fans and deltas, for
504 instance in seismic datasets, where only delta channel network angles have been quantified before
505 (Mahon et al., 2024). Our results confirm the prior modern data (Chakraborty et al., 2010) and recent
506 modeling outcomes (Martin & Edmonds, 2023), and help to eliminate a conundrum or discrepancy in
507 plan-view versus cross-sectional fluvial fan facies models (Plink-Björklund, 2021). Namely, earlier work
508 suggested bifurcations as a key mechanism driving fluvial fan formation (Friend, 1978; Kelly & Olsen,
509 1993; Weissman et al., 2010), probably due to downstream channel narrowing. However, this hypothesis
510 contradicts the stratigraphic data that indicate that proximal fans consist of amalgamated channel deposits
511 (Chakraborty et al., 2010; Kelly & Olsen, 1993; Nichols & Fisher, 2007; Singh et al., 1993; Weissman et
512 al., 2013) – a pattern consistent with frequent avulsions (Chakraborty et al., 2010; Singh et al., 1993).

513 **5.4 Sensitivity of Deltas and Fluvial Fans to Global Change**

514 Deltas and fluvial fans differ significantly in their vulnerability to natural hazards and in their
515 responses to global change. Deltas are highly vulnerable to coastal hazards and sea level rise (e.g.,
516 Syvitski et al., 2009; Giosan et al., 2014). Rising sea-level will not only inundate deltaic distributary
517 networks, but also cause a landward migration of the avulsion node corresponding with the landward shift
518 of the backwater zone (Chatanantavet et al., 2012; Ganti et al., 2014). This process reduces sediment
519 delivery to shorelines accelerating the effects of sea-level rise. In contrast, fluvial fans are controlled by
520 upstream morphodynamics, where the fan location (apex) is pinned by a topographic break (Ganti et al.,
521 2014; Martin & Edmonds, 2023). While sea-level rise and coastal erosion would affect the fan toes, the
522 avulsion node and fan apex position, and sediment delivery would not be affected, making fluvial fans
523 significantly less vulnerable to drowning.

524 Both deltas and fluvial fans are affected by reduced sediment supply due to river damming and
525 artificial levees (e.g., Blum & Roberts, 2009; Syvitski et al., 2009; Giosan et al., 2014; Nienhuis et al.,
526 2020; Paola et al., 2011). However, fluvial fans are highly sensitive to the water and sediment supply



527 changes, such as driven by changes in precipitation patterns (Leier et al., 2005; Assine et al., 2014;
528 Hansford & Plink-Björklund, 2020). Increases in extreme precipitation cause a significant increase in
529 avulsion frequency and crevassing splay formation (Morón et al., 2017), because large fluctuations in
530 river discharge, such as during extreme precipitation events, are avulsion-triggering events (Jones &
531 Schumm, 1999). Indeed, fluvial fans have been shown to be highly sensitive to such changes, where
532 fluvial fan activation and deactivation cycles have been linked to millennial-scale changes in monsoon
533 intensity or precipitation pattern (Assine et al., 2014; Fontana et al., 2014, Latrubblesse et al., 2012).

534

535 **6. Conclusions**

536 This study demonstrates that river-dominated delta and fluvial fan channel networks can be
537 distinguished using quantitative morphometric criteria derived from their channel network topology.
538 Deltaic networks are primarily shaped by bifurcation processes resulting in average bifurcation angles of
539 approximately 74° , consistent with diffusion-dominated growth. In contrast, fluvial fan topology is
540 shaped by channel avulsions producing narrower average network angles near 55° , indicative of surface
541 runoff processes. Fluvial fan network angles tend to widen downstream, likely due to decreasing gradients
542 and avulsion style shifts, while delta angles remain relatively consistent, reflecting persistent bifurcation
543 processes. Both channel networks display downstream reductions in channel length and width with
544 increasing channel order, but the fluvial fan networks are characterized by significantly longer and
545 somewhat narrower channels when normalized.

546 These differences not only support the use of network morphology as a diagnostic tool for
547 identifying ancient fluvial fans and deltas in the stratigraphic record or other planetary bodies but also
548 provide insights into their differing sensitivities to environmental change.

549

550 **Code Availability**

551 The Python code used for data analysis and figure generation was created and run in Jupyter
552 Notebook version 6.4.8 (Anaconda distribution).

553

554 **Data Availability**

555 Morphological data collected in this study are available at <https://github.com/lukegezovich/Delta-and->
556 [Fluvial-Fan-Networks](https://github.com/lukegezovich/Delta-and-Fluvial-Fan-Networks).

557

558 **Competing Interests**

559 The authors declare that they have no conflict of interest.

560



561 **Acknowledgments**

562 We thank reviewers Drs. Kamini Singha, Lesli Wood, and Wendy Zhou for their constructive
563 feedback that helped improve earlier versions of this manuscript.

564

565 **Financial Support**

566 Luke Gezovich thanks the American Association of Petroleum Geologists (AAPG) Foundation
567 John & Erika Lockridge Grant, the American Institute of Professional Geologists (AIPG) William J. Siok
568 Graduate Scholarship, the Colorado Scientific Society (CSS), the Rocky Mountain Association of
569 Geologists (RMAG), and the Society for Sediment Geology (SEPM) for providing funding to support this
570 research.

571

572

573

574

575

576

577

578

579

580

581

582

583

584

585

586

587



588 **References**

589 Allen, P. A. (2008). Time scales of tectonic landscapes and their sediment routing systems. *Geological*
590 *Society, London, Special Publications*, 296(1), 7–28. <https://doi.org/10.1144/SP296.2>

591 Assine, M. L., Corradini, F. A., Pupim, F. D. N., & McGlue, M. M. (2014). Channel arrangements and
592 depositional styles in the São Lourenço fluvial megafan, Brazilian Pantanal wetland. *Sedimentary*
593 *Geology*, 301, 172–184. <https://doi.org/10.1016/j.sedgeo.2013.11.007>

594 Bates, C. C. (1953). Rational Theory of Delta Formation. *AAPG Bulletin*, 37.
595 <https://doi.org/10.1306/5CEADD76-16BB-11D7-8645000102C1865D>

596 Blair, T. C., & McPherson, J. G. (1994). Alluvial Fans and their Natural Distinction from Rivers Based on
597 Morphology, Hydraulic Processes, Sedimentary Processes, and Facies Assemblages. *SEPM Journal of*
598 *Sedimentary Research*, Vol. 64A. <https://doi.org/10.1306/D4267DDE-2B26-11D7-8648000102C1865D>

599 Bramble, M. S., Goudge, T. A., Milliken, R. E., & Mustard, J. F. (2019). Testing the deltaic origin of fan
600 deposits at Bradbury Crater, Mars. *Icarus*, 319, 363–366. <https://doi.org/10.1016/j.icarus.2018.09.024>

601 Broaddus, C. M., Vulis, L. M., Nienhuis, J. H., Tejedor, A., Brown, J., Foufoula-Georgiou, E., & Edmonds, D.
602 A. (2022). First-Order River Delta Morphology Is Explained by the Sediment Flux Balance From Rivers,
603 Waves, and Tides. *Geophysical Research Letters*, 49(22). <https://doi.org/10.1029/2022GL100355>

604 Brooke, S., Chadwick, A. J., Silvestre, J., Lamb, M. P., Edmonds, D. A., & Ganti, V. (2022). Where rivers
605 jump course. *Science*, 376(6596), 987–990. <https://doi.org/10.1126/science.abm1215>

606 Bryant, M., Falk, P., & Paola, C. (1995). Experimental study of avulsion frequency and rate of deposition.
607 *Geology*, 23(4), 365. [https://doi.org/10.1130/0091-7613\(1995\)023<0365:ESOAFA>2.3.CO;2](https://doi.org/10.1130/0091-7613(1995)023<0365:ESOAFA>2.3.CO;2)

608 Chakraborty, T., Kar, R., Ghosh, P., & Basu, S. (2010). Kosi megafan: Historical records, geomorphology
609 and the recent avulsion of the Kosi River. *Quaternary International*, 227(2), 143–160.
610 <https://doi.org/10.1016/j.quaint.2009.12.002>

611 Chatanantavet, P., Lamb, M. P., & Nittrouer, J. A. (2012). Backwater controls of avulsion location on
612 deltas. *Geophysical Research Letters*, 39(1), 2011GL050197. <https://doi.org/10.1029/2011GL050197>

613 Chen, C., Tian, B., Schwarz, C., Zhang, C., Guo, L., Xu, F., Zhou, Y., & He, Q. (2021). Quantifying delta
614 channel network changes with Landsat time-series data. *Journal of Hydrology*, 600, 126688.
615 <https://doi.org/10.1016/j.jhydrol.2021.126688>

616 Coffey, T. S., & Shaw, J. B. (2017). Congruent Bifurcation Angles in River Delta and Tributary Channel
617 Networks. *Geophysical Research Letters*, 44(22). <https://doi.org/10.1002/2017GL074873>

618 Davidson, S. K., & Hartley, A. J. (2014). A Quantitative Approach To Linking Drainage Area and
619 Distributive-Fluvial-System Area In Modern and Ancient Endorheic Basins. *Journal of Sedimentary*
620 *Research*, 84(11), 1005–1020. <https://doi.org/10.2110/jsr.2014.79>

621 Davidson, S. K., Hartley, A. J., Weissmann, G. S., Nichols, G. J., & Scuderi, L. A. (2013). Geomorphic
622 elements on modern distributive fluvial systems. *Geomorphology*, 180–181, 82–95.
623 <https://doi.org/10.1016/j.geomorph.2012.09.008>



624 De Toffoli, B., Plesa, A. -C., Hauber, E., & Breuer, D. (2021). Delta Deposits on Mars: A Global Perspective.
625 *Geophysical Research Letters*, 48(17), e2021GL094271. <https://doi.org/10.1029/2021GL094271>

626 Devauchelle, O., Petroff, A. P., Seybold, H. F., & Rothman, D. H. (2012). Ramification of stream networks.
627 *Proceedings of the National Academy of Sciences*, 109(51), 20832–20836.
628 <https://doi.org/10.1073/pnas.1215218109>

629 Edmonds, D. A., Martin, H. K., Valenza, J. M., Henson, R., Weissmann, G. S., Miltenberger, K., Mans, W.,
630 Moore, J. R., Slingerland, R. L., Gibling, M. R., Bryk, A. B., & Hajek, E. A. (2022). Rivers in reverse:
631 Upstream-migrating dechannelization and flooding cause avulsions on fluvial fans. *Geology*, 50(1), 37–
632 41. <https://doi.org/10.1130/G49318.1>

633 Edmonds, D. A., Paola, C., Hoyal, D. C. J. D., & Sheets, B. A. (2011). Quantitative metrics that describe
634 river deltas and their channel networks. *Journal of Geophysical Research*, 116(F4), F04022.
635 <https://doi.org/10.1029/2010JF001955>

636 Edmonds, D. A., & Slingerland, R. L. (2007). Mechanics of river mouth bar formation: Implications for the
637 morphodynamics of delta distributary networks. *Journal of Geophysical Research: Earth Surface*,
638 112(F2), 2006JF000574. <https://doi.org/10.1029/2006JF000574>

639 Fagherazzi, S., Edmonds, D. A., Nardin, W., Leonardi, N., Canestrelli, A., Falcini, F., Jerolmack, D. J.,
640 Mariotti, G., Rowland, J. C., & Slingerland, R. L. (2015). Dynamics of river mouth deposits. *Reviews of
641 Geophysics*, 53(3), 642–672. <https://doi.org/10.1002/2014RG000451>

642 Federici, B., & Paola, C. (2003). Dynamics of channel bifurcations in noncohesive sediments. *Water
643 Resources Research*, 39(6), 2002WR001434. <https://doi.org/10.1029/2002WR001434>

644 Fielding, C. R., Ashworth, P. J., Best, J. L., Prokocki, E. W., & Smith, G. H. S. (2012). Tributary, distributary
645 and other fluvial patterns: What really represents the norm in the continental rock record? *Sedimentary
646 Geology*, 261–262, 15–32. <https://doi.org/10.1016/j.sedgeo.2012.03.004>

647 Fontana, A., Mozzi, P., & Marchetti, M. (2014). Alluvial fans and megafans along the southern side of the
648 Alps. *Sedimentary Geology*, 301, 150–171. <https://doi.org/10.1016/j.sedgeo.2013.09.003>

649 Friend, P. F. (1978). *DISTINCTIVE FEATURES OF SOME ANCIENT RIVER SYSTEMS*.

650 Galloway, E. (1975). Process Framework for Describing the Morphologic and Stratigraphic Evolution of
651 Deltaic Depositional Systems. *Deltas: Models for Exploration*, 1975, 87–98.

652 Ganti, V., Chu, Z., Lamb, M. P., Nittrouer, J. A., & Parker, G. (2014). Testing morphodynamic controls on
653 the location and frequency of river avulsions on fans versus deltas: Huanghe (Yellow River), China.
654 *Geophysical Research Letters*, 41(22), 7882–7890. <https://doi.org/10.1002/2014GL061918>

655 Gearon, J. H., Martin, H. K., DeLisle, C., Barefoot, E. A., Mohrig, D., Paola, C., & Edmonds, D. A. (2024).
656 Rules of river avulsion change downstream. *Nature*, 634(8032), 91–95. [https://doi.org/10.1038/s41586-024-07964-2](https://doi.org/10.1038/s41586-
657 024-07964-2)

658 Gupta, N., Dahal, S., Kumar, A., Kumar, C., Kumar, M., Maharjan, A., Mishra, D., Mohanty, A., Navaraj, A.,
659 Pandey, S., Prakash, A., Prasad, E., Shrestha, K., Shrestha, M. S., Subedi, R., Subedi, T., Tiwary, R.,
660 Tuladhar, R., & Unni, A. (2021). Rich water, poor people: Potential for transboundary flood management



661 between Nepal and India. *Current Research in Environmental Sustainability*, 3, 100031.
662 <https://doi.org/10.1016/j.crsust.2021.100031>

663 Hariharan, J., Piliouras, A., Schwenk, J., & Passalacqua, P. (2022). Width-Based Discharge Partitioning in
664 Distributary Networks: How Right We Are. *Geophysical Research Letters*, 49(14), e2022GL097897.
665 <https://doi.org/10.1029/2022GL097897>

666 Hartley, A. J., Weissmann, G. S., Nichols, G. J., & Warwick, G. L. (2010). Large Distributive Fluvial Systems:
667 Characteristics, Distribution, and Controls on Development. *Journal of Sedimentary Research*, 80(2),
668 167–183. <https://doi.org/10.2110/jsr.2010.016>

669 Horton, B. K., & Decelles, P. G. (2001). *Modern and ancient Fluvial megafans in the foreland basin system
670 of the central Andes, southern Bolivia: Implications for drainage network evolution in fold-thrust belts*
671 (pp. 43–63).

672 Isikdogan, F., Bovik, A., & Passalacqua, P. (2017). RivaMap: An automated river analysis and mapping
673 engine. *Remote Sensing of Environment*, 202, 88–97. <https://doi.org/10.1016/j.rse.2017.03.044>

674 Jerolmack, D. J., & Swenson, J. B. (2007). Scaling relationships and evolution of distributary networks on
675 wave-influenced deltas. *Geophysical Research Letters*, 34(23), 2007GL031823.
676 <https://doi.org/10.1029/2007GL031823>

677 Jones, L. S., & Schumm, S. A. (1999). Causes of Avulsion: An Overview. In N. D. Smith & J. Rogers (Eds.),
678 *Fluvial Sedimentology VI* (1st ed., pp. 169–178). Wiley. <https://doi.org/10.1002/9781444304213.ch13>

679 Ke, W., Shaw, J. B., Mahon, R. C., & Cathcart, C. A. (2019). Distributary Channel Networks as Moving
680 Boundaries: Causes and Morphodynamic Effects. *Journal of Geophysical Research: Earth Surface*, 124(7),
681 1878–1898. <https://doi.org/10.1029/2019JF005084>

682 Kelly, S. B., & Olsen, H. (1993). Terminal fans a review with reference to Devonian examples. In
683 *Sedimentary Geology* (Vol. 85, pp. 339–374).

684 Lauzon, R., Piliouras, A., & Rowland, J. C. (2019). Ice and Permafrost Effects on Delta Morphology and
685 Channel Dynamics. *Geophysical Research Letters*, 46(12), 6574–6582.
686 <https://doi.org/10.1029/2019GL082792>

687 Leier, A. L., DeCelles, P. G., & Pelletier, J. D. (2005). Mountains, monsoons, and megafans. *Geology*,
688 33(4), 289. <https://doi.org/10.1130/G21228.1>

689 Limaye, A. B., Adler, J. B., Moodie, A. J., Whipple, K. X., & Howard, A. D. (2023). Effect of Standing Water
690 on Formation of Fan-Shaped Sedimentary Deposits at Hypanis Valles, Mars. *Geophysical Research
691 Letters*, 50(4), e2022GL102367. <https://doi.org/10.1029/2022GL102367>

692 Mahon, R., Hughes, C., Chen, H., & Shaw, J. (2024). Ancient Channel-Mouth Bifurcation Angles on Earth
693 and Mars. *The Sedimentary Record*, 22(1). <https://doi.org/10.2110/001c.124824>

694 Martin, H. K., & Edmonds, D. A. (2023). Avulsion dynamics determine fluvial fan morphology in a cellular
695 model. *Geology*, 51(8), 796–800. <https://doi.org/10.1130/G51138.1>



696 Morais, E. S., & Montanher, O. C. (2022). Avulsion in a meandering river: Floodplain conditions for
697 occurrence and effects in the parent channel. *CATENA*, 214, 106236.
698 <https://doi.org/10.1016/j.catena.2022.106236>

699 Morón, S., Amos, K., Edmonds, D. A., Payenberg, T., Sun, X., & Thyer, M. (2017). Avulsion triggering by El
700 Niño–Southern Oscillation and tectonic forcing: The case of the tropical Magdalena River, Colombia. *GSA
701 Bulletin*, 129(9–10), 1300–1313. <https://doi.org/10.1130/B31580.1>

702 Moscariello, A. (2018). Alluvial fans and fluvial fans at the margins of continental sedimentary basins:
703 Geomorphic and sedimentological distinction for geo-energy exploration and development. *Geological
704 Society, London, Special Publications*, 440(1), 215–243. <https://doi.org/10.1144/SP440.11>

705 Nichols, G. J., & Fisher, J. A. (2007). Processes, facies and architecture of fluvial distributary system
706 deposits. *Sedimentary Geology*, 195(1–2), 75–90. <https://doi.org/10.1016/j.sedgeo.2006.07.004>

707 Nienhuis, J. H., Ashton, A. D., & Giosan, L. (2015). What makes a delta wave-dominated? *Geology*, 43(6),
708 511–514. <https://doi.org/10.1130/G36518.1>

709 Nienhuis, J. H., Hoitink, A. J. F. T., & Törnqvist, T. E. (2018). Future Change to Tide-Influenced Deltas.
710 *Geophysical Research Letters*, 45(8), 3499–3507. <https://doi.org/10.1029/2018GL077638>

711 North, C. P., & Warwick, G. L. (2007). Fluvial Fans: Myths, Misconceptions, and the End of the Terminal-
712 Fan Model. *Journal of Sedimentary Research*, 77(9), 693–701. <https://doi.org/10.2110/jsr.2007.072>

713 Paniagua-Arroyave, J. F., & Nienhuis, J. H. (2024). The Quantified Galloway Ternary Diagram of Delta
714 Morphology. *Journal of Geophysical Research: Earth Surface*, 129(11), e2024JF007878.
715 <https://doi.org/10.1029/2024JF007878>

716 Passalacqua, P. (2017). The Delta Connectome: A network-based framework for studying connectivity in
717 river deltas. *Geomorphology*, 277, 50–62. <https://doi.org/10.1016/j.geomorph.2016.04.001>

718 Pearson, S. G., Van Prooijen, B. C., Elias, E. P. L., Vitousek, S., & Wang, Z. B. (2020). Sediment
719 Connectivity: A Framework for Analyzing Coastal Sediment Transport Pathways. *Journal of Geophysical
720 Research: Earth Surface*, 125(10), e2020JF005595. <https://doi.org/10.1029/2020JF005595>

721 Piliouras, A., Lauzon, R., & Rowland, J. C. (2021). Unraveling the Combined Effects of Ice and Permafrost
722 on Arctic Delta Morphodynamics. *Journal of Geophysical Research: Earth Surface*, 126(4),
723 e2020JF005706. <https://doi.org/10.1029/2020JF005706>

724 Plink-Björklund, P. (2021). Distributive Fluvial Systems: Fluvial and Alluvial Fans. In *Encyclopedia of
725 Geology* (pp. 745–758). Elsevier. <https://doi.org/10.1016/B978-0-08-102908-4.00015-1>

726 Rahman, M. M., Howell, J. A., & MacDonald, D. I. M. (2022). Quantitative analysis of crevasse-splay
727 systems from modern fluvial settings. *Journal of Sedimentary Research*, 92(9), 751–774.
728 <https://doi.org/10.2110/jsr.2020.067>

729 Reitz, M. D., & Jerolmack, D. J. (2012). Experimental alluvial fan evolution: Channel dynamics, slope
730 controls, and shoreline growth. *Journal of Geophysical Research: Earth Surface*, 117(F2), 2011JF002261.
731 <https://doi.org/10.1029/2011JF002261>

732 Schumm, S. A. (1977). The fluvial system. *Food and Agriculture Organization of the United Nations*.



733 Schwanghart, W., & Kuhn, N. J. (2010). TopoToolbox: A set of Matlab functions for topographic analysis.
734 *Environmental Modelling & Software*, 25(6), 770–781. <https://doi.org/10.1016/j.envsoft.2009.12.002>

735 Seybold, H. J., Kite, E., & Kirchner, J. W. (2018). Branching geometry of valley networks on Mars and
736 Earth and its implications for early Martian climate. *Science Advances*, 4(6), eaar6692.
737 <https://doi.org/10.1126/sciadv.aar6692>

738 Seybold, H., Rothman, D. H., & Kirchner, J. W. (2017). Climate's watermark in the geometry of stream
739 networks. *Geophysical Research Letters*, 44(5), 2272–2280. <https://doi.org/10.1002/2016GL072089>

740 Singh, H., Parkash, B., & Gohain, K. (1993). Facies analysis of the Kosi megafan deposits. *Sedimentary
741 Geology*, 85(1–4), 87–113. [https://doi.org/10.1016/0037-0738\(93\)90077-1](https://doi.org/10.1016/0037-0738(93)90077-1)

742 Slingerland, R., & Smith, N. D. (1998). Necessary conditions for a meandering-river avulsion. *Geology*,
743 26(5), 435. [https://doi.org/10.1130/0091-7613\(1998\)026<0435:NCFAMR>2.3.CO;2](https://doi.org/10.1130/0091-7613(1998)026<0435:NCFAMR>2.3.CO;2)

744 Tebolt, M., & Goudge, T. A. (2022). Global investigation of martian sedimentary fan features: Using
745 stratigraphic analysis to study depositional environment. *Icarus*, 372, 114718.
746 <https://doi.org/10.1016/j.icarus.2021.114718>

747 Tejedor, A., Longjas, A., Edmonds, D. A., Zaliapin, I., Georgiou, T. T., Rinaldo, A., & Foufoula-Georgiou, E.
748 (2017). Entropy and optimality in river deltas. *Proceedings of the National Academy of Sciences*, 114(44),
749 11651–11656. <https://doi.org/10.1073/pnas.1708404114>

750 Tejedor, A., Longjas, A., Zaliapin, I., & Foufoula-Georgiou, E. (2015). Delta channel networks: 1. A graph-
751 theoretic approach for studying connectivity and steady state transport on deltaic surfaces. *Water
752 Resources Research*, 51(6), 3998–4018. <https://doi.org/10.1002/2014WR016577>

753 Törnqvist, T. E., & Bridge, J. S. (2002). Spatial variation of overbank aggradation rate and its influence on
754 avulsion frequency. *Sedimentology*, 49(5), 891–905. <https://doi.org/10.1046/j.1365-3091.2002.00478.x>

755 Vulis, L., Tejedor, A., Ma, H., Nienhuis, J. H., Broaddus, C. M., Brown, J., Edmonds, D. A., Rowland, J. C., &
756 Foufoula-Georgiou, E. (2023). River Delta Morphotypes Emerge From Multiscale Characterization of
757 Shorelines. *Geophysical Research Letters*, 50(7), e2022GL102684.
758 <https://doi.org/10.1029/2022GL102684>

759 Walker, H. J. (1998). Arctic Deltas. *Journal of Coastal Research*, 14(3), 718–738.

760 Weissman, G. S., Hartley, A. J., Nichols, G. J., Scuderi, L. A., Olson, M., Buehler, H., & Banteah, R. (2010).
761 *Fluvial form in modern continental sedimentary basins: Distributive fluvial systems*.
762 <https://doi.org/10.1016/j.jgeo>

763 Weissmann, G. S., Hartley, A. J., Scuderi, L. A., Nichols, G. J., Owen, A., Wright, S., Felicia, A. L., Holland,
764 F., & Anaya, F. M. L. (2015). Fluvial geomorphic elements in modern sedimentary basins and their
765 potential preservation in the rock record: A review. *Geomorphology*, 250, 187–219.
766 <https://doi.org/10.1016/j.geomorph.2015.09.005>

767 Wolinsky, M. A., Edmonds, D. A., Martin, J., & Paola, C. (2010). Delta allometry: Growth laws for river
768 deltas. *Geophysical Research Letters*, 37(21), 2010GL044592. <https://doi.org/10.1029/2010GL044592>



769 Wright, L. D. (1977). Sediment transport and deposition at river mouths: A synthesis. *Geological Society*
770 *of America Bulletin*, 88(6), 857. [https://doi.org/10.1130/0016-7606\(1977\)88<857:STADAR>2.0.CO;2](https://doi.org/10.1130/0016-7606(1977)88<857:STADAR>2.0.CO;2)

771 Yang, H. (2020). Numerical investigation of avulsions in gravel-bed braided rivers. *Hydrological*
772 *Processes*, 34(17), 3702–3717. <https://doi.org/10.1002/hyp.13837>

773

774